Temporal dissociation between local and global functional adaptations of the maternal brain to childbirth: A longitudinal assessment

Short title:

Temporal dissociation between local and global functional adaptations of maternal brain

Natalia Chechko[1,2,3,*], Susanne Nehls[2,3], Elena Losse[2], Juergen Dukart[1,4], Leon D. Lotter[1,4,5,*]

[1]Institute of Neuroscience and Medicine, Brain & Behavior (INM-7), Research Center Jülich, Jülich 52428, Germany
[2]Department of Psychiatry, Psychotherapy and Psychosomatics, Medical Faculty, RWTH Aachen, Aachen 52074, Germany
[3]Institute of Neuroscience and Medicine, JARA-Institute Brain Structure Function Relationship (INM 10), Research Center Jülich, Jülich 52428, Germany
[4]Institute of Systems Neuroscience, Medical Faculty, Heinrich Heine University Düsseldorf, Düsseldorf 40225, Germany
[5]Max Planck School of Cognition, Stephanstrasse 1A, Leipzig 04103, Germany

*Corresponding authors:
nchechko@ukaachen.de
l.lotter@fz-juelich.de

Abstract

The early peripartum period and motherhood are associated with significant physiological and psychological challenges. Despite the acknowledged relevance of the maternal brain's postpartum reorganization of functional activity and connectivity, the dynamics of these changes are yet to be adequately understood. We sought to assess healthy maternal brain function longitudinally across 6 consecutive time points within a 24-week period after childbirth, beginning in the first postpartum week. The resting-state functional magnetic resonance imaging (rsfMRI) data of 98 women (75 postpartum and 23 nulliparous) with 189 MRI sessions revealed a general dissociation between local and global functional connectivity (FC) and activity measures. In postpartum women, we observed persistently altered intraregional activity and connectivity throughout the 6 postpartum months. In contrast, the reduced whole-brain FC of the subcortical areas was found to normalize to control levels about 6 to 9 weeks postpartum. This dissociation between the temporal trajectories of postpartum local and global rsfMRI connectivity changes indicates diverging underlying biological mechanisms. Given the massive hormone fluctuations that occur in the first few weeks postpartum, the transient brain function changes within this period may be hormone-related. On the other hand, the long-lasting functional changes of the maternal brain may be linked to permanent processes such as behavioral or psychological adaptations to pregnancy and childbirth. Although the latter hypothesis requires further testing, our findings add significantly to the understanding of healthy maternal brain function, affording valuable insight into the atypical adaptation processes, and potentially opening up new avenues for the study of postpartum psychiatric disorders.

Introduction

The biological and psychological adaptations that pregnancy and the early postpartum period trigger in the maternal brain are testament to the neuroplasticity of the adult brain. Within the first few days of delivery, the maternal brain structure, with widespread changes in gray matter volume (GMV) and cortical thickness across all lobes, differs markedly from that of nulliparous controls [1]. Particularly noteworthy in the distinction between the maternal and nulliparous brains is the prominent role of the left amygdala [2]. Thought to be mediated by sex steroid hormones and corticosteroids [3,4], these morphometric changes follow temporal trajectories with the most dynamic changes occurring in the first 6 weeks postpartum [2]. However, the GMV in the dorsomedial prefrontal cortex and the cortical thickness of the subgenual and lateral prefrontal cortices may not normalize to pre-pregnancy levels even at 12 weeks postpartum [2,5,6]. As these findings indicate, pregnancy and childbirth/motherhood may have regionally divergent short-term and long-term effects on the brain. While the biological role of these effects is not adequately understood, it has been suggested that they may play a role in maternal attachment toward the offspring [2,5,7].

In comparison to the effects of pregnancy and childbirth on brain morphology, their effects on brain activity and neural network organization are under-investigated. It is conceivable, however, that brain function undergoes substantial restructuring in pregnancy and the postpartum period given the abovementioned changes in brain morphology, the massive hormonal adaptations in the perinatal period [3,8], the reported hormonal regulation of brain connectivity [9,10], and the interactions between sex hormones and GABAergic as well as oxytonergic neurotransmission [11,12]. Resting-state functional magnetic resonance imaging (rsfMRI) provides a simple-to-perform, easily scalable, compliance- and performance-independent tool to gain insights into the peripartum reorganization of brain function [13]. Longitudinal study designs with multiple postpartum scans are necessary to examine potential regionally divergent short- and long-term alterations of brain function associated with pregnancy and childbirth. A previous rsfMRI study [14] had reported changes in the default mode network (DMN) temporal coherence in the cuneus at about 1 to 4 months

postpartum compared to pre-conception. The elaborate applied study design with one pre-pregnancy and one postpartum scan allowed the authors to investigate the long-term effects of pregnancy on resting-state functional connectivity (FC). However, a set of follow-up data with a high temporal resolution might be better suited to evaluate the brain's functional reorganization in the context of the massive physiological adaptation in the early postpartum period, and to disentangle the short-term biological effects of pregnancy and the early postpartum phase from those of motherhood (Stickel et al., 2023). Voxel- or cluster-level MRI inferences allow only limited conclusions with respect to the potential involvement of biological mechanisms in the observed MRI alterations. Spatial colocalization analyses that quantify the degree of alignment between (i) observed MRI maps and (ii) a biological system of interest can help redress this limitation [15–17]. Applied to single-subject MRI maps, this approach has been successfully used to study physiological structural changes in the brain during the development of and pathophysiological alterations in Parkinson's and Huntington's diseases [17,18].

Using rsfMRI, we assessed healthy maternal brain function longitudinally across 6 consecutive time points within a 24-week period after childbirth. Beginning in the first postpartum week, the assessments continued, at 3-week intervals, for 12 weeks, with a final assessment at week 24 postpartum. Assessments of serum estradiol and progesterone were also made during this period. We hypothesized that, compared to their nulliparous counterparts (NP), postpartum women (PP) would show strong alterations of the rsfMRI metrics mapping intra- and interregional brain activity and FC. Given the high temporal resolution of our study's longitudinal design, we sought to distinguish the transitory rsfMRI changes from the long-lasting ones. In order to test the hypothesis that brain activity and connectivity are influenced by hormone-mediated processes, we (i) determined whether whole-brain distributions of rsfMRI activity and connectivity changes colocalized with spatial distributions of hormone receptors and the functionally-related neurotransmitter receptors, and (ii) assessed the time-dependent covariance between rsfMRI changes and blood plasma estradiol and progesterone levels at each rsfMRI session. Based on the hypothesis that

permanent changes in brain function may be associated with psychological and/or behavioral changes due to motherhood [2,5,7], we examined whether these functional adaptations in the brain covaried with mother-infant attachment and maternal depression levels over time.

Results

Demographic, hormonal, and psychological assessments

The data of 98 women, 75 PP and 23 NP, with 189 MRI sessions were included in the analyses, which evaluated postpartum reorganization of intra- and interregional rsfMRI activity and connectivity. All participants were examined at baseline (T0; PP: mean = 3.43, SD = 2.03 days postpartum) with between 17 and 19 PP subjects undergoing up to 5 subsequent longitudinal assessments (T1–T5). The longitudinal subgroup was measured at 6.2 (SD = 2.24) (T0), 22.42 (SD = 2.52) (T1), 43.57 (SD = 3.06) (T2), 64.61 (SD = 2.8) (T3), 84.91 (SD = 3.71) (T4), and 173.32 days (10.15) (T5) postpartum. Baseline sample characteristics are presented in supplementary Tables S1 and S2. The PP group (mean age: 30.52, SD = 3.54) and the NP group (mean age: 28.04, SD = 4.91) differed in age (Mann-Whitney-U-Test, U = 1075.5, $p < .001$).

The longitudinal effects of hormone levels, psychological variables, and fMRI-derived measures were tested for the linear mixed models (LMM), making use of all follow-up data. The fixed effect of postpartum week (continuous variable) was modeled on each tested response variable, accounting for the within-subject variance. For each response variable, two mixed linear models were calculated: (i) including only the linear postpartum week as fixed effect and (ii) including the linear and quadratic effects.

As regards the blood hormone levels, we found a quadratic effect of time on log-transformed progesterone levels, but not on estradiol or the estradiol/progesterone ratio. Maternal attachment [Maternal Postnatal Attachment Scale, MPAS; ,19] and sub-clinical postpartum depression scores [Edinburgh Postnatal Depression Scale, EPDS; ,20] showed linear and quadratic effects of time (nominal $p < 0.05$; Table S3).

Strong regional alterations of resting-state activity and connectivity in the first postpartum week

To identify brain areas showing robust adaptation effects of pregnancy and childbirth, we followed a comprehensive rsfMRI analysis approach, simultaneously assessing postpartum changes in voxel-level *intra*-regional/local rsfMRI activity (fractional amplitude of low frequency fluctuations, fALFF), *intra*-regional/local FC (Local Correlation, LCOR), as well as *inter*-regional/global FC (Global Correlation, GCOR) [21–23]. To determine rsfMRI changes occurring in the first postpartum week, which were to be monitored in subsequent longitudinal analyses, we compared the rsfMRI metrics between baseline PP and NP groups in general linear models (GLM) controlling for age (non-parametric cluster-level inference: voxel-level threshold $p < .01$, cluster-level threshold $p < .05$). For all analyses, effect sizes are presented in addition to statistical significance estimates based on non-parametric permutation procedures.

We found two clusters with increased local activity (fALFF) in PP relative to NP in the right precentral and left medial temporal areas, and one cluster with decreased local activity in the right superior frontal gyrus. For LCOR, PP showed two relatively symmetric clusters of decreased local connectivity in the bilateral insula compared to controls. In contrast, GCOR was decreased in PP relative to NP in two symmetric subcortical clusters covering parts of the bilateral putamen and pallidum (Table 1, Figure 1). In sensitivity analyses, the results were robust against additional control for in-scanner motion, GMV, and education (Table S4).

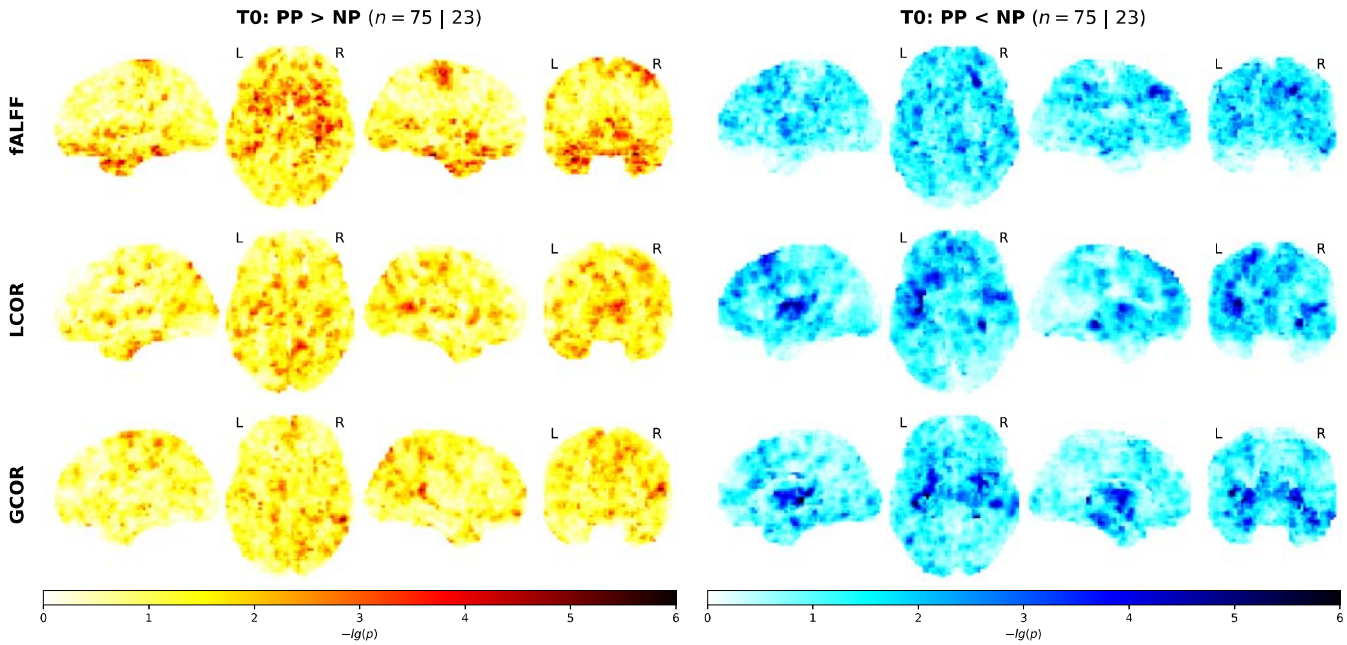

Figure 1. Clusters of differing local activity (fALFF), local connectivity (LCOR), and global connectivity (GCOR) in the nulliparous (NP) and postpartum (PP) groups at baseline.

Cluster-level and whole-brain results from baseline (T0) rsfMRI analyses. Brain maps for each rsfMRI metric (rows) and each contrast (columns) show voxel-level negative log10-transformed p values overlaid by cluster-level results in darker shades (non-parametric cluster mass permutation). Abbreviations: PP = postpartum, NP = nulliparous, fALFF = fractional amplitude of low frequency fluctuations, LCOR = local correlation, GCOR = global correlation.

Table 1. Statistical and anatomical characteristics of baseline rsfMRI clusters.

Measure	Contrast	Cluster name	X	Y	Z	-lg(p)	Cluster size [mm^3]	AAL region coverage
fALFF	PP > NP	rightPrecentral	40	-20	60	1.43	3672	72.06% Precentral_R; 22.79% Postcentral_R
		leftMedTemp	-29	10	-36	1.37	3321	47.97% Temporal_Pole_Mid_L; 19.51% ParaHippocampal_L; 16.26% Temporal_Inf_L; 8.13% Temporal_Pole_Sup_L
		rightPFC	22	37	45	1.31	2835	80.95% Frontal_Sup_2_R; 14.29% Frontal_Mid_2_R
LCOR	PP < NP	leftIns	-41	-17	9	2.23	11124	36.89% Insula_L; 32.52% Rolandic_Oper_L; 9.95% Heschl_L; 7.77% Temporal_Sup_L
		rightIns	43	-2	6	1.44	5481	57.64% Insula_R; 25.62% Rolandic_Oper_R; 9.85% no_label
GCOR		leftPut	-26	-2	3	1.78	5724	71.23% Putamen_L; 20.28% Pallidum_L; 8.02% no_label
		rightPut	28	-5	3	1.6	5373	63.32% Putamen_R; 16.08% Pallidum_R; 13.57% no_label; 7.04% Insula_R

Note. Clusters were named after their main location. X, Y, and Z show coordinates in MNI-152 space. The non-parametric p value associated with each cluster based on its cluster mass is displayed negative log10 transformed. Clusters were characterized anatomically based on the AAL atlas in terms of the percentage to which each AAL region was contained in each cluster.

Abbreviations: AAL = Automated Anatomic Labeling atlas, fALFF = fractional amplitude of low frequency fluctuations, LCOR = local correlation, GCOR = global correlation, PP = postpartum, NP = nulliparous, MED = medial, PFC = prefrontal cortex, Ins = insula, Put = putamen.

Temporal dissociation of intra- and interregional rsfMRI metrics in the postpartum period

To examine the longitudinal patterns of the observed early postpartum rsfMRI changes, we extracted the average rsfMRI signal from each of the significant baseline clusters. Independent t-tests at each time point were used to determine “normalization” of rsfMRI metrics relative to the NP control group. As described above, the longitudinal development was tested in LMMs with the differences between individual time points being assessed by means of post-hoc paired t-tests.

We found a general dissociation between local measures (fALFF and LCOR) and the global connectivity measure (GCOR) (Figure 2, Tables S5–7). As regards the former, we observed persistently altered intraregional activity and connectivity in PP across the 6 observed postpartum months. In contrast, the reduced whole-brain FC of the subcortical areas showed normalization patterns, with no significant or visible group differences between PP and NP at about 6-9 weeks postpartum (FDR-corrected). In line with that, only the GCOR clusters showed significant linear and quadratic longitudinal development (FDR-corrected). As shown by the longitudinal rsfMRI sensitivity analyses (Tables S8–10), controlling for the underlying GMV reduced the effect sizes, while the group differences and longitudinal trends remained stable.

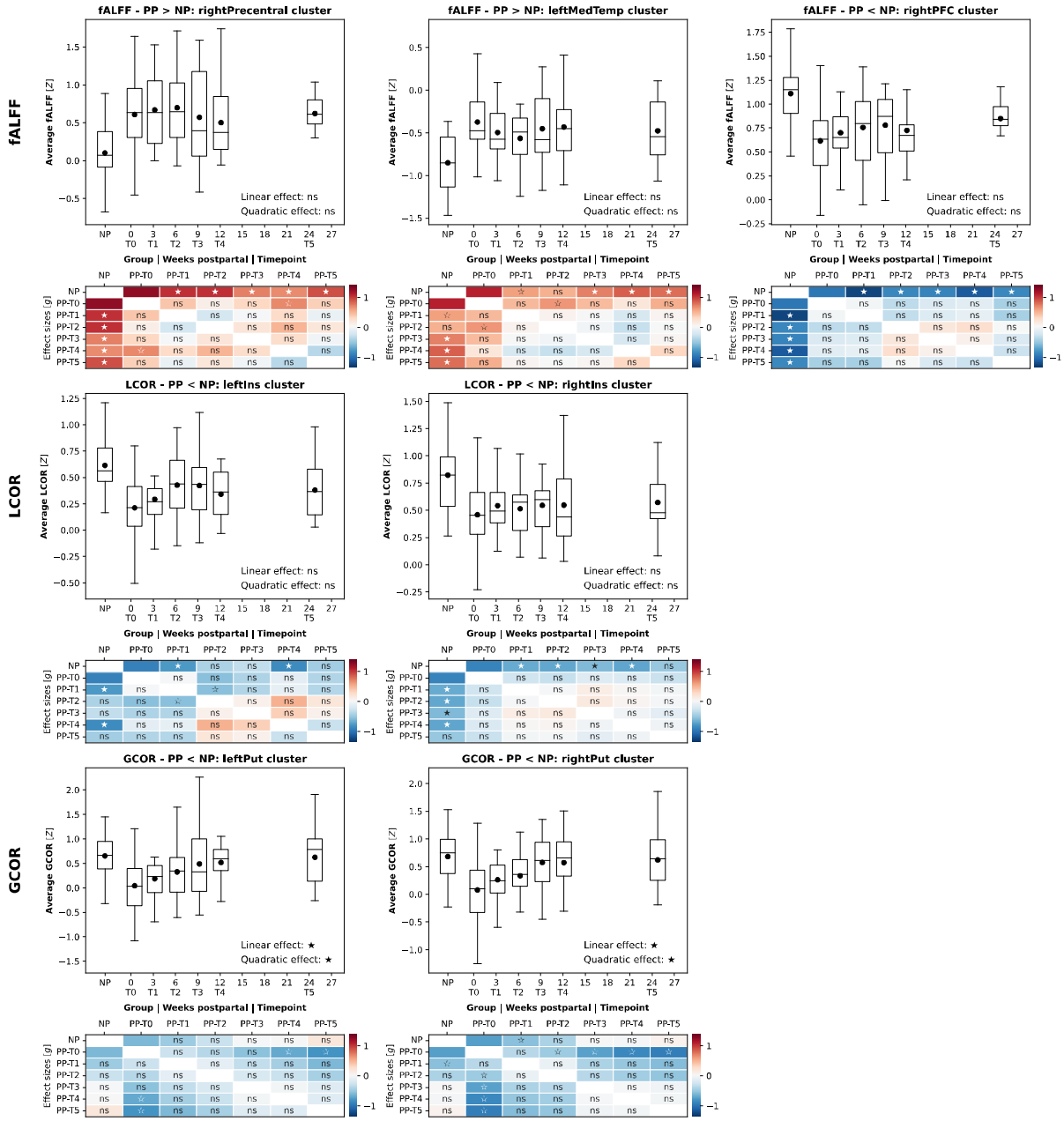

Figure 2. Longitudinal development of rsfMRI clusters.

Development of baseline cluster-wise averaged local and global connectivity and activity metrics across 6 postpartum months. Boxplots: x-axes show time in weeks postpartum (dimensional scale), y-axes show the Z-standardized rsfMRI metric. Each dot represents one subject at one individual time point, lines connect longitudinal scans. Boxplots show the distribution across subjects at each time point (black dot = mean, middle line = median, boxes = quartile 1 and 3, whiskers = range if below 1.5 * interquartile range from quartile 1 or 3). Heatmaps show effect sizes (Hedge's g) of within- and between-group comparisons, overlaid labels mark significances (filled star = false discovery-corrected, empty star = nominal p < .05, ns = p > .05. Significance of linear mixed models is printed in the lower left corner. Abbreviations: fALFF = fractional amplitude of low frequency fluctuations, LCOR = local correlation, GCOR = global correlation, PP = postpartum, NP = nulliparous, ns = not significant.

Whole-brain rsfMRI changes colocalize with potentially mediating biological systems

If the change of a brain function metric is influenced by a brain system on another organizational level, the spatial distribution of this metric across the brain may colocalize with the brain system in question [16,18,24]. We therefore examined if rsfMRI changes and their normalization in PP relative to NP were distributed across the brain following spatial distributions of pregnancy-specific hormonal receptors (progesterone: PGR, estrogen: ESR1/ESR2, cortisol: NR3C1/NR3C2) and functionally-related neurotransmitter receptors (oxytocin: OXTR, GABA: $GABA_A$, glutamate: mGluR5). In-vivo maps of $GABA_A$ and mGluR5 distributions were obtained with positron emission tomography imaging in independent healthy adult subjects [25,26], all other maps were derived from postmortem Allen Brain Atlas data [27] (Figure 3, left). We tested for colocalization between (i) parcellated rsfMRI maps of each PP subject relative to the NP group and (ii) the independent receptor maps using Spearman correlations [28]. In case of a significant group-average colocalization at baseline (FDR-corrected), we evaluated the temporal development at each subsequent time point.

Baseline changes of fALFF in PP relative to NP were positively colocalized with progesterone (FDR-corrected) and estrogen receptor distributions (nominal $p < .05$), but negatively colocalized with the metabotropic glutamate receptor distribution (FDR-corrected; Figure 3, upper right; Table S11). In line with cluster-level results reported above, both the fALFF-PGR and fALFF-mGluR5 colocalization persisted across the first 6 postpartum months (Figure 3, lower right; Table S11–12). LCOR changes showed spatial colocalization with estrogen, cortisol, and glutamate receptors (nominal $p < 0.05$). While the GCOR changes colocalized positively with cortisol receptors (NR3C1: nominal, NR3C2: FDR) and $GABA_A$ (nominal), they did so negatively with progesterone and oxytocin receptors (FDR). Again, in line with the cluster-level results, these colocalization patterns normalized within the first 2 postpartum months.

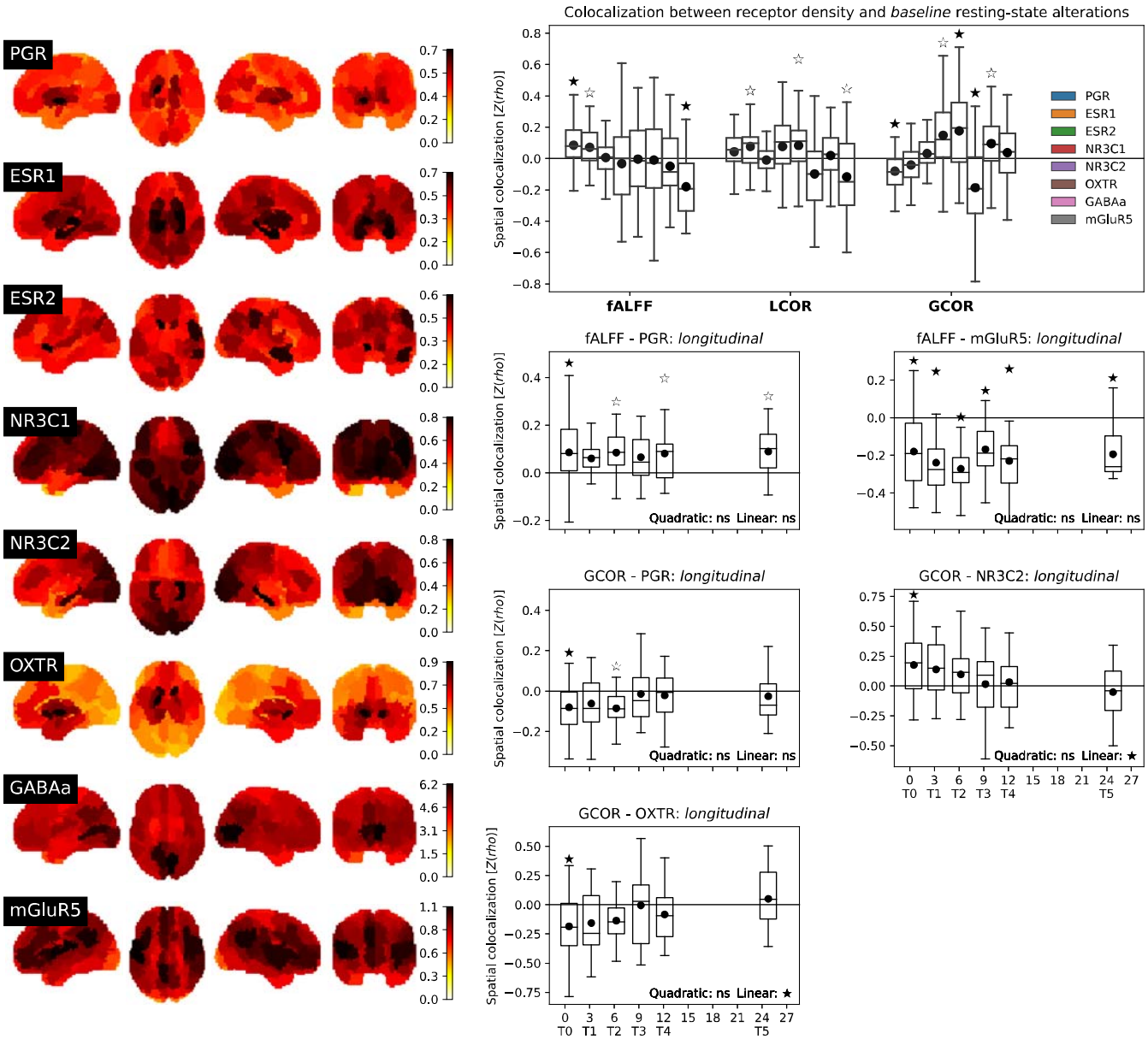

Figure 3. Subject-level spatial colocalization between postpartum rsfMRI alterations and hormonal/neurotransmitter receptor densities.

Left side: Parcellated and Z-standardized whole-brain hormone and neurotransmitter receptor distributions. Right side: Spatial colocalization analyses. Upper panel: Baseline analyses testing for colocalization between receptor distributions and rsfMRI data of each postpartum subject at baseline relative to the control group. X-axis: Z-transformed Spearman correlation coefficients, y-axis: rsfMRI metrics, colors: receptor maps. Lower panels: Longitudinal analyses following up on each baseline results if associated group permutation p values survived false discovery rate-correction (filled stars). The plot design equals Figure 2 with the y axis showing Z-transformed Spearman correlation coefficients. Abbreviations: fALFF = fractional amplitude of low frequency fluctuations, LCOR = local correlation, GCOR = global correlation, ns = not significant.

Receptor distributions provide a multivariate explanation of postpartum rsfMRI changes

To provide an easy-to-interpret quantification of the extent to which postpartum rsfMRI changes could be explained by hormone and neurotransmitter receptor distributions, we assessed the variance explained in multivariate linear regression analyses "predicting" baseline subject-level rsfMRI change patterns in PP from receptor maps [15,16]. On average, baseline rsfMRI change patterns in PP were explained to 17.1% for fALFF (range 0 – 43.8%), 13.0% for LCOR (range 0 – 38.1%), and 18.3% for GCOR (0 – 44.0%).

Early postpartum normalization of global connectivity is not due to regression-to-the-mean effects

We further tested if normalization effects observed in GCOR-related variables might be due to regression-toward-the-mean effects. For this, we (i) replicated baseline voxel-level GLM and spatial colocalization analyses while *excluding* the subjects with longitudinal data, (ii) extracted cluster-average data from subjects *with* longitudinal data using the clusters estimated on the independent cross-sectional sample, and (iii) tested for longitudinal linear and quadratic effects in the cluster-average data.

The reduced PP sample (n = 56) showed the same bilateral putamen-related clusters of reduced global connectivity at baseline. Temporal development of the cluster-average data in independent longitudinal subjects followed the trajectory as reported above. Baseline spatial colocalization patterns in the reduced sample were similar to those in the full sample (Figure S1, Table S13).

Temporally dissociated intra- and interregional rsfMRI metric changes show diverging behavioral and hormonal association patterns

The dissociation between the temporal trajectories of postpartum local and global rsfMRI connectivity changes indicates diverging underlying biological mechanisms. Given the first postpartum weeks' strong hormonal fluctuations, it is plausible that the transient changes of brain function within this time frame are hormone-related, while the long-lasting changes may be linked to more permanent processes such as behavioral or psychological adaptations to

pregnancy and childbirth. Due to our rather small sample size, we conducted hormonal and behavioral association analyses on an exploratory level, evaluating general patterns rather than specific associations. To fully exploit our dense longitudinal data, we fitted LMMs testing for the interaction effect of postpartum weeks and MRI variables (cluster-level and spatial colocalization metrics) on both the behavioral and hormonal variables (hormone levels, EPDS, and MPAS).

This resulted in the emergence of two general patterns (Figure 4). First, the GCOR-derived metrics seemed to be generally associated with the hormone levels (Table S14). This was in line with the temporal development observed in the GCOR-related variables and the hypothesis that postpartum adaptations of global connectivity are driven by changes in corticosteroid hormones. In contrast, postpartum depression symptoms (EPDS) and mother-child attachment (MPAS) seemed to be more associated with the local resting-state metrics, suggesting a potential behavioral correlate for persistent changes in postpartum brain function (Table S15). We maintain, however, that these findings are of a preliminary nature and would require targeted evaluation in an independent sample.

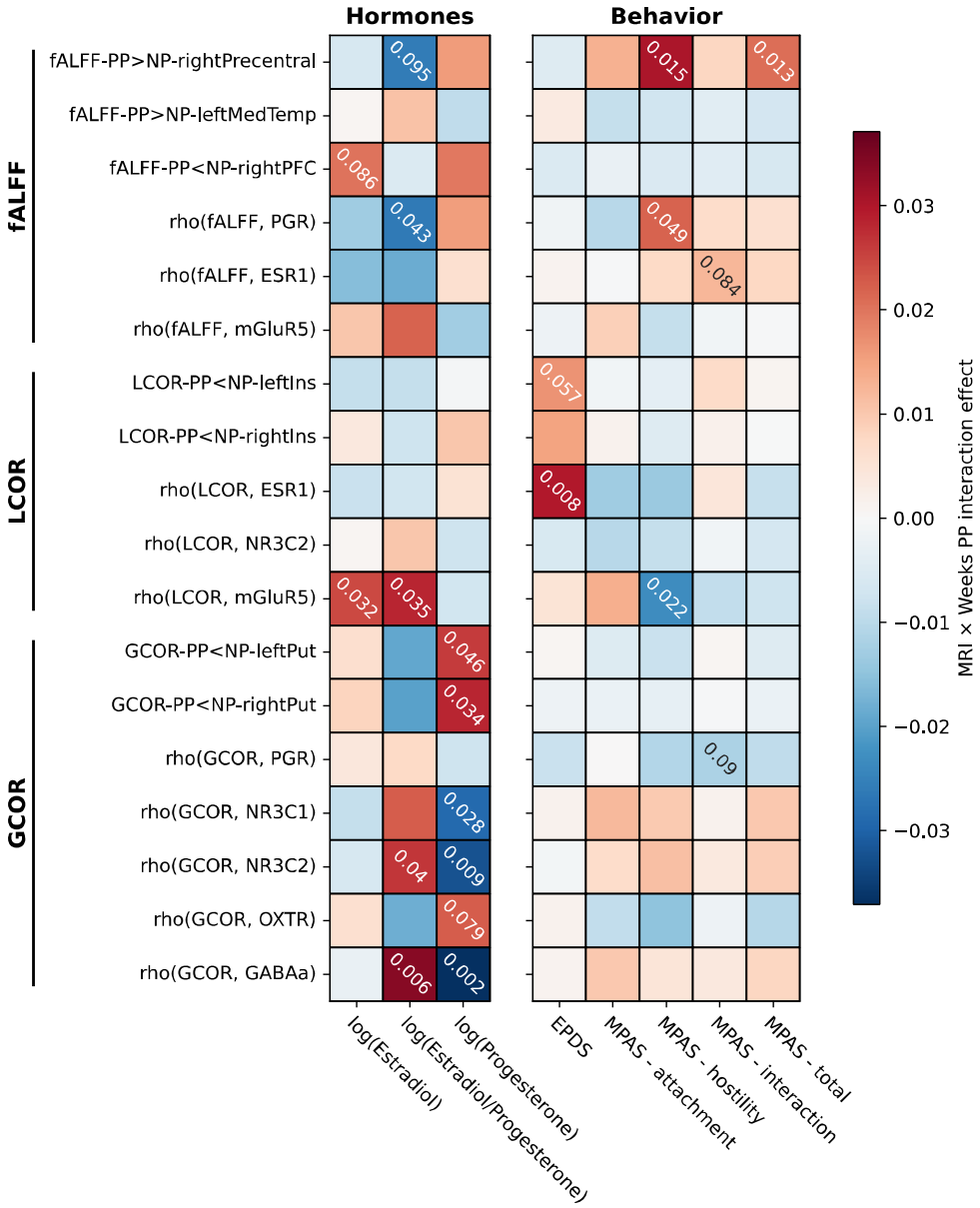

Figure 4. Patterns of association over time between rsfMRI results and hormone levels as well as behavior.

Results of linear mixed models to determine time-dependent covariation between rsfMRI metrics (cluster-level and spatial colocalization estimates) and hormone levels (left) as well as mother-child attachment and postpartum depression symptoms (right). Heatmap colors represent standardized effect sizes of the MRI x postpartum week interaction effect. Overlaid labels show nominal p values ($p < 0.1$). The shown analyses are intended to identify general patterns of associations, rather than interpreting specific tests. Abbreviations: fALFF = fractional amplitude of low frequency fluctuations, LCOR = local correlation, GCOR = global correlation, PP = postpartum, NP = nulliparous, MPAS = Maternal Postnatal Attachment Scale, EPDS = Edinburgh Postnatal Depression Scale.

Discussion

A healthy postpartum sample was recruited within one week of childbirth and was subjected to frequent longitudinal rsfMRI sampling over the first 24 postpartum weeks, which revealed temporal milestones in the perinatal and postpartum reorganization of brain function. Strong alterations of intra- and interregional resting-state activity and connectivity were detected in the first post-childbirth week. Whole-brain connectivity of the subcortical regions normalized to control levels within the first 2 postpartum months, likely mediated by adaptations of the steroid hormone systems. In contrast, intraregional changes in the precentral, the prefrontal, the medial temporal and insular cortices persisted throughout the entire follow-up period, with indications of links to glutamatergic neurotransmission and maternal behavior. Notably, we found the rsfMRI alterations to persist when controlling for the underlying GMV, indicating partly independent mechanisms influencing postpartum reorganization of the brain's structure [2] and function.

The subacute postpartum period: Transient effects of pregnancy and childbirth on global rsfMRI connectivity

After about 6 to 9 postpartum weeks, we could not detect significant group differences in the subcortical global connectivity between PP and NP. Spatial colocalization analyses suggested that these temporary connectivity change patterns on the whole-brain level might be explained by the spatial distribution of progesterone, cortisol, and $GABA_A$ receptors. The temporal normalization trajectories covaried with changes in the progesterone levels.

The so-called acute/subacute postpartum period (comprising the first 6 postpartum weeks) is characterized by processes involving extensive physiological and hormonal adaptation [29]. Alterations of the bilateral putamen FC during this period showed the largest effect sizes in this study. This, in line with previous research, suggests positive effects of progesterone on neural function and the GMV of basal ganglia and putamen [30]. With respect to mood, steroid hormones are also thought to have effects on the basal ganglia and other parts of the reward system [31].

In vulnerable women, the decrease in the levels of progesterone and progesterone metabolites following childbirth was hypothesized to be involved in the development of baby blues and postpartum depression via the dysregulation of GABAergic neurotransmission [32]. In healthy women, the likely progesterone-dependent decrease in global FC shortly after delivery, followed by a quick restoration, may be a worthwhile research target in the context of the development of postpartum depression. However, despite the magnitude of the physiological adaptations, they are inconsequential for most postpartum mothers, with factors such as life experiences and genetic predisposition likely contributing to their susceptibility to hormonal fluctuations [33]. Therefore, the neuroendocrine effects on mood must be understood in the context of individual risk factors. As we included only non-depressed women, further studies would be needed to understand how the changes in postpartum functional connectivity are linked to changes in mood in women with increased susceptibility to depression.

Beyond the subacute postpartum period: does pregnancy prime the brain?

What remains as yet unclear is when the post-pregnancy recovery of the maternal brain is completed, and if pregnancy has long-lasting neural effects. The postnatal adaptation processes involving structural change appear to start quite early in the postpartum phase [34,35], lasting up to 6 months [34] or even longer [5,36]. We found the changes in local activity of the motor, medial temporal, and prefrontal cortices, as well as local FC in the bilateral insulae, to remain persistently altered throughout the first 6 postpartum months. FALFF was found to be stronger in the regions with higher progesterone and estrogen receptor density, and lower in areas with higher glutamate receptor density, suggesting that the long-term effects of pregnancy are mediated by these hormones. Notably, these local activity metrics did not show any normalization patterns, possibly indicating associations with persistent postnatal physiological and behavioral changes. A link was seen between the local resting-state estimates and the postnatal behavioral data, within which a potential link between the insular connectivity and mother-child attachment would require further investigation [37,38].

In a study with a unique design, Hoekzema et al. [14] have also reported long-term effects of pregnancy or motherhood on resting-state connectivity, indicating that motherhood may permanently increase temporal coherence within the DMN. Focusing primarily on the adaptations occurring in the very early postpartum period and in early motherhood, our data help further extend the understanding of pregnancy-related effects on the maternal brain. According to our findings, the brain's functional and structural adaptations involve highly dynamic temporal changes in the first 12 postpartum weeks [2], an important time frame for hormonal, metabolic and behavioral adaptations [29], which was not covered by Hoekzema et al.

It is not only pregnancy and childbirth, but also the experience of motherhood that shapes the maternal brain, with the time factor likely playing a major role. For instance, in a related study using partly the same dataset, we observed that amygdala volume changes over 9 to 12 postpartum weeks predicted less hostile behavior toward the child, with no such association seen at an earlier postpartum stage [2]. In addition, an inverse relationship has been suggested between functional connectivity in older women (as opposed to men) and the number of children parented, indicating neuroprotective effects of motherhood on brain function in later life [6]. From this point of view, the effects reported by Hoekzema et al. [14] may indeed be seen as being due to motherhood, with stronger DMN changes in the study found to be associated with the quality of mother-infant bonding. The same may be true for the associations seen in the present study between local rsfMRI metrics and maternal behavior.

Limitations

As regards the interpretation of our findings, several limitations ought to be pointed, the most important one being the lack of a longitudinal follow-up in the control group. However, we consider the comparisons with the nulliparous group to be robust, as relevant changes in the nulliparous brain are unlikely given the relatively short follow-up duration. In addition, due to the lack of pre-pregnancy and during-pregnancy rsfMRI, we cannot disentangle the effects of pregnancy from those of postpartum adaptation or any preexisting factor. For a longitudinal

study of postpartum neuroplasticity, the group size of 19 women is sufficient, although behavioral and hormonal association patterns need to be replicated in larger groups. All in all, we consider this study to be a reliable blueprint for hypothesis generation with respect to a homogeneous group of healthy postpartum women. Finally, the inferences from spatial colocalization analyses were limited by virtue of having been related mostly to receptor density source data, which had been acquired partly from male postmortem samples.

Conclusion and future outlook

We provide the first evidence of temporally dynamic adaptation processes in the early postpartum brain. While the subcortex-centered global connectivity changes may be of transient nature and are related to hormonal adaptations, neocortical brain activity and connectivity show persistent alterations, possibly associated with behavioral and psychological processes. Further longitudinal studies involving larger cohorts and pre-pregnancy assessments may afford valuable insights into the post-childbirth recovery of pregnancy-affected brain morphology and function. Along with longitudinal multimodal neuroimaging, cognitive and lifestyle assessments, the tracking of ovarian hormones from before pregnancy through the postpartum phase can help identify factors that contribute to the phenomena observed in this study. It is imperative to understand the long-term effects of pregnancy-related adaptations, which, in addition to playing a protective role, may also render women more vulnerable to certain risks. It needs to be ascertained if these changes contribute to the development of psychiatric conditions, especially in women at higher risks for postpartum psychiatric disorders.

Methods

Participants

Prior to enrolment in the study, written informed consent was obtained from each participant. The study, which conformed to the Helsinki declaration, was approved by the Ethics Committee of the University Hospital RWTH Aachen.

The data of 75 non-depressed postpartum women were included in MRI processing. Postpartum women were recruited within 1 to 7 days of childbirth (T0) in the Department of Gynecology and Obstetrics, University Hospital Aachen. From this sample, 19 PP women took part in longitudinal MRI assessments, with measurements at 3 weeks (T1, n = 19), 6 weeks (T2, n = 18), 9 weeks (T3, n = 19), 12 weeks (T4, n = 19) and 24 weeks (T5, n = 17) postpartum. At each time point, blood samples were drawn to determine blood plasma levels of estradiol and progesterone. PP participants were assessed for symptoms of postpartum depression by means of the EPDS [20] (T0–T5, total score) and for mother-child attachment through the MPAS (T1–T5, total score and sub-scores for quality of attachment, absence of hostility, and pleasure in interaction).

23 healthy nulliparous women with no history of psychiatric disorders were included as a control group, scanned once with the same scanner.

We excluded sessions that exceeded motion cut-offs of a mean and maximum framewise displacement of 0.5 and 3 mm, respectively, as well as one session with MRI data reconstruction failure. The final dataset consisted of data from 98 subjects (PP = 75, NP = 23) with overall 189 sessions (longitudinal: T0: 19, T1: 19, T2: 18, T3: 19, T4: 18, T5: 17).

Hormonal assays

Progesterone and estradiol serum concentrations were measured before each scanning session and analyzed by competitive immunometry electrochemistry luminescence detection at the Laboratory Diagnostic Center, University Hospital RWTH Aachen, Germany. The samples were run on a Roche Cobas e601 and on a Roche Cobas e801 with Cobas Elecsys estradiol and progesterone reagent kits, respectively (Roche Diagnostics, Bromma, Sweden). For progesterone, the measurement interval was .05–60 ng/ml with an intra-assay coefficient of variation of 2.33–2.49%. For estradiol, the measurement interval was 5–3000 pg/ml with a coefficient of variation of 1.77–2.91%.

Software, external data sources, and code availability

The processing of functional and structural images was conducted in a MATLAB (R2022a) environment using CONN (21a) [39], building on routines from SPM12 (https://www.fil.ion.ucl.ac.uk/spm/software/spm12/). The statistical analyses were calculated in a Python (3.9.12) environment with Nilearn (0.10.0) [40] being used for the voxel-wise rsfMRI group comparisons. The resulting spatial clusters were characterized using atlasreader (0.1.2) [41]. Spatial colocalization estimates were calculated in JuSpyce (0.0.3) [28]. All post-hoc statistical analyses were conducted with statsmodels (0.13.5) and pingouin (0.5.3) [42,43]. Brain gene expression and nuclear imaging data were obtained with abagen (0.1.3) [44], neuromaps (0.0.3) [45], and from author sources [25,26]. Visualizations were created with matplotlib (3.5.2) [46], seaborn (0.12.1) [47], and nilearn.

The analysis code, organized in a Jupyter notebook, is available as a supplement to this manuscript. Due to privacy protection, we cannot provide subject data openly. All group-level results are provided in supplementary tables. Group-level MRI volumes will be uploaded to Neurovault following publication.

MRI processing

The preprocessing of functional images consisted of removal of the first four frames, realignment for motion correction, and co-registration to structural images with subsequent spatial normalization into Montreal Neurological Institute space using parameters derived from structural data. The normalization parameters were applied with modulation to segmented gray matter probability maps to obtain corresponding voxel-wise GMV. Functional and structural images were interpolated to 3-mm and 1-mm isotopic resolution, respectively. A Gaussian smoothing kernel of 6-mm full width at half maximum was applied to rsfMRI data. Twenty-four motion parameters along with mean white matter and cerebrospinal fluid signals were regressed out of the functional data [48]. The resulting images were linearly detrended and temporally bandpass filtered (0.01–0.08 Hz). A gray matter mask (probability > 0.2) was applied to all images to restrict analyses to gray matter tissue. For spatial colocalization analyses, data were parcellated into 100 cortical and 16

subcortical parcels [49,50]. All structural and functional MRI volumes before and after preprocessing were visually quality-controlled.

RsfMRI analyses at baseline

We assessed postpartum changes of voxel-level intraregional/local rsfMRI activity (fALFF) and connectivity (LCOR) as well as interregional/global connectivity (GCOR). For descriptions of these metrics, please refer to Lotter et al. [23].

To identify spatial clusters of altered regional functional connectivity and activity in mothers after childbirth, we compared voxel-wise metrics between the baseline PP and NP groups. We fitted GLMs including age as a covariate. Cluster-level significance was determined in separate positive (PP > NP) and negative contrasts (PP < NP) based on the permutation of cluster masses (10,000 iterations) using a voxel-level threshold of $p < .01$ and a cluster-level threshold of $p < .05$ [51].

Longitudinal rsfMRI analyses

To assess how rsfMRI changes at baseline developed during the first 6 postpartum months**,** we extracted average rsfMRI data for each cluster and assessed (i) differences between PP and HC at each time point using ANCOVAs controlled for age, (ii) longitudinal development in PP using LMMs, and (iii) within-subject differences between time points in multiple paired t-tests. FDR-correction was applied to all p values resulting from each analysis (separately for step i, ii, and iii). LMMs were designed to assess the fixed effect of postpartum week on each MRI metric, while accounting for within-subject variance. In sensitivity analyses, we included average signals within the same clusters, as extracted from modulated gray matter maps as covariates [23].

Spatial colocalization between voxel-wise rsfMRI changes and receptor distributions

We examined whether changes in the rsfMRI metrics in PP relative to NP displayed patterns across the whole brain that were present in receptor distributions that were likely functionally related [24]. The presence of these spatial relationships could indicate potential involvement of the respective receptor in the observed rsfMRI changes [18,24]. We first assessed if the

mean spatial colocalization of rsfMRI changes in PP at baseline exceeded those of permutated null data. RsfMRI-receptor combinations that showed significant colocalization at baseline were followed up in the longitudinal data.

Corticosteroid hormone and oxytocin receptor maps (PGR, ESR1/ESR2, NR3C1/NR3C2, OXTR) were constructed from postmortem Allen Brain Atlas gene expression data (1 female, ages 24.0–57.0 years, mean = 42.50, SD = 13.38) [27] in 116-region volumetric atlas space. The abagen toolbox was used for map construction, while applying bilateral mirroring across hemispheres. GABAergic ($GABA_A$) and glutamatergic (mGluR5) receptor maps were obtained with positron emission tomography from independent groups of healthy adult subjects ($GABA_A$: [11C]flumazenil, n = 10, mean = 26.60, SD = 7.00 years; mGluR5: [11C]ABP688, n = 73, mean = 19.90, SD = 3.04 years).

Spatial relationships were tested for by (i) parcellating all rsfMRI and receptor data in 116 cortical and subcortical parcels, (ii) calculating parcel-wise rsfMRI Z scores for each PP subject at a given time point by subtraction of the mean rsfMRI metric in NP subjects and division by the NP standard deviation, (iii) correlating these subject-level 116-parcel Z score maps with each receptor map using Spearman correlations, (iv) generating a null distribution of Spearman correlation coefficients by repeating this process after permuting the PP-NP labels, and (v) fitting a Gaussian curve to these null distributions to estimate the p value of each observed Spearman correlation ("colocalization") coefficient. The concept was described in detail in Dukart et al. [24] and implemented via JuSpyce[28] . The Gaussian curve was fitted to generate p values with enough decimal places to accurately apply FDR correction. If significant colocalization was observed on the group level at baseline, the longitudinal development of these colocalization metrics was tested for using LMMs as described above.

Additionally, to quantify the extent to which whole-brain rsfMRI changes in PP at baseline were explained by the receptor maps in an easily interpretable way, we fitted multivariate linear models "predicting" subject-wise rsfMRI changes in PP from all receptor maps as

independent variables [15,16]. We quantified the outcome as the average adjusted R^2 across the PP sample.

Analyses of MRI, hormone, and behavior associations

To evaluate potential physiological and behavioral correlates of temporal trajectories observed in the rsfMRI data, we fitted LMMs evaluating the MRI metric vs. weeks postpartum interaction effect on hormonal and behavioral variables (log-transformed progesterone, estrogen, and progesterone/estrogen ratio, as well as MPAS and EPDS total scores and MPAS sub-scale scores). Given the small sample size of the longitudinal sample, these analyses were conducted on an exploratory level, evaluating patterns rather than specific associations. To allow for this, results where visualized as a heatmap focusing on effect sizes.

Acknowledgments

This work was supported by the Brain Imaging Facility of the Interdisciplinary Center for Clinical Research (IZKF) Aachen within the Faculty of Medicine at RWTH Aachen University. Leon D. Lotter received financial support from the Max Planck Society (MPG) and the German Ministry of Education and Research (BMBF), Germany.

Funding

The study was funded by the Rotation Program (2015–2017) of the Medical Faculty of the University Hospital RWTH Aachen, and the Deutsche Forschungsgemeinschaft (DFG, No. 410314797 and No. 512021469).

References

1. Chechko N, Dukart J, Tchaikovski S, Enzensberger C, Neuner I, Stickel S. The expectant brain – pregnancy Leads to changes in brain morphology in the early postpartum period. Cereb Cortex. 2021; 2021.06.29.450283. doi:10.1093/cercor/bhab463
2. Nehls S, Losse E, Enzensberger C, Frodl T, Chechko N. Time-sensitive changes in the maternal brain and their influence on mother-child attachment. Transl Psychiatry. 2023.
3. Galea LAM, Frokjaer VG. Perinatal depression: embracing variability toward better treatment and outcomes. Neuron. 2019;102: 13–16. doi:10.1016/j.neuron.2019.02.023

4. Sacher J, Chechko N, Dannlowski U, Walter M, Derntl B. The peripartum human brain: Current understanding and future perspectives. Front Neuroendocrinol. 2020;59: 100859. doi:10.1016/j.yfrne.2020.100859

5. Hoekzema E, Barba-Müller E, Pozzobon C, Picado M, Lucco F, García-García D, et al. Pregnancy leads to long-lasting changes in human brain structure. Nat Neurosci. 2017;20: 287–296. doi:10.1038/nn.4458

6. Orchard ER, Ward PGD, Chopra S, Storey E, Egan GF, Jamadar SD. Neuroprotective effects of motherhood on brain function in late life: A resting-state fMRI study. Cereb Cortex. 2021;31: 1270–1283. doi:10.1093/cercor/bhaa293

7. Kim P, Leckman JF, Mayes LC, Feldman R, Wang X, Swain JE. The plasticity of human maternal brain: Longitudinal changes in brain anatomy during the early postpartum period. Behav Neurosci. 2010;124: 695–700. doi:10.1037/a0020884

8. Lindsay JR, Nieman LK. The hypothalamic-pituitary-adrenal axis in pregnancy: Challenges in disease detection and treatment. Endocr Rev. 2005;26: 775–799. doi:10.1210/er.2004-0025

9. Peper JS, van den Heuvel MP, Mandl RCW, Pol HEH, van Honk J. Sex steroids and connectivity in the human brain: A review of neuroimaging studies. Psychoneuroendocrinology. 2011;36: 1101–1113. doi:10.1016/J.PSYNEUEN.2011.05.004

10. Andreano JM, Touroutoglou A, Dickerson B, Barrett LF. Hormonal Cycles, Brain Network Connectivity, and Windows of Vulnerability to Affective Disorder. Trends Neurosci. 2018;41: 660–676. doi:10.1016/J.TINS.2018.08.007

11. Barth C, Villringer A, Sacher J. Sex hormones affect neurotransmitters and shape the adult female brain during hormonal transition periods. Front Neurosci. 2015;9: 37. doi:10.3389/fnins.2015.00037

12. Ivell R, Walther N. The role of sex steroids in the oxytocin hormone system. Mol Cell Endocrinol. 1999;151: 95–101. doi:10.1016/S0303-7207(99)00025-8

13. Damoiseaux JS, Rombouts SARB, Barkhof F, Scheltens P, Stam CJ, Smith SM, et al. Consistent resting-state networks across healthy subjects. Proc Natl Acad Sci. 2006;103: 13848–13853. doi:10.1073/pnas.0601417103

14. Hoekzema E, van Steenbergen H, Straathof M, Beekmans A, Freund IM, Pouwels PJWW, et al. Mapping the effects of pregnancy on resting state brain activity, white matter microstructure, neural metabolite concentrations and grey matter architecture. Nat Commun. 2022;13: 6931. doi:10.1038/s41467-022-33884-8

15. Hansen JY, Shafiei G, Markello RD, Smart K, Cox SML, Nørgaard M, et al. Mapping neurotransmitter systems to the structural and functional organization of the human neocortex. Nat Neurosci. 2022;25: 1569–1581. doi:10.1038/s41593-022-01186-3

16. Lotter LD, Saberi A, Hansen JY, Misic B, Barker GJ, Bokde ALW, et al. Human cortex development is shaped by molecular and cellular brain systems. bioRxiv Prepr Serv Biol. 2023 [cited 18 Jul 2023]. doi:10.1101/2023.05.05.539537

17. Dukart J, Holiga S, Rullmann M, Lanzenberger R, Hawkins PCT, Mehta MA, et al. JuSpace□: A tool for spatial correlation analyses of magnetic resonance imaging data with nuclear imaging derived neurotransmitter maps. Hum Brain Mapp. 2021;42: 555–566. doi:10.1002/hbm.25244

18. Kasper J, Eickhoff SB, Caspers S, Peter J, Dogan I, Wolf RC, et al. Local synchronicity in dopamine-rich caudate nucleus influences Huntington's disease motor phenotype. Brain. 2023. doi:10.1093/brain/awad043

19. Condon JT, Corkindale CJ. The assessment of parent-to-infant attachment: development of a self-report questionnaire instrument. J Reprod Infant Psychol. 1998;16: 57–76.

20. Cox JL, Holden JM, Sagovsky R. Detection of postnatal depression. Development of the 10-item Edinburgh Postnatal Depression Scale. Br J Psychiatry. 1987;150: 782–786. Available: http://www.ncbi.nlm.nih.gov/pubmed/3651732

21. Zou Q-H, Zhu C-Z, Yang Y, Zuo X-N, Long X-Y, Cao Q-J, et al. An improved approach to detection of amplitude of low-frequency fluctuation (ALFF) for resting-state fMRI: fractional ALFF. J Neurosci Methods. 2008;172: 137–141.

22. Whitfield-Gabrieli S, Nieto-Castanon A. Conn□: A Functional Connectivity Toolbox for Correlated and Anticorrelated Brain Networks. Brain Connect. 2012;2: 125–141. doi:10.1089/brain.2012.0073

23. Lotter LD, von Polier G, Offermann J, Buettgen K, Stanetzky L, Eickhoff SB, et al. Recovery-Associated Resting-State Activity and Connectivity Alterations in Anorexia Nervosa. Biol Psychiatry Cogn Neurosci Neuroimaging. 2021;6: 1023–1033. doi:10.1016/j.bpsc.2021.03.006

24. Dukart J, Holiga S, Rullmann M, Lanzenberger R, Hawkins PCT, Mehta MA, et al. JuSpace□: A tool for spatial correlation analyses of magnetic resonance imaging data with nuclear imaging derived neurotransmitter maps. Hum Brain Mapp. 2021;42: 555–566. doi:10.1002/hbm.25244

25. Kaulen N, Rajkumar R, Régio Brambilla C, Mauler J, Ramkiran S, Orth L, et al. mGluR5 and GABAA receptor-specific parametric PET atlas construction—PET/MR data processing pipeline, validation, and application. Hum Brain Mapp. 2022;43: 2148–2163. doi:10.1002/HBM.25778

26. Smart K, Cox SML, Scala SG, Tippler M, Jaworska N, Boivin M, et al. Sex differences in [11 C]ABP688 binding: a positron emission tomography study of mGlu5 receptors. Eur J Nucl Med Mol Imaging. 2019;46: 1179–1183. doi:10.1007/S00259-018-4252-4/FIGURES/2

27. Hawrylycz MJ, Lein ES, Guillozet-Bongaarts AL, Shen EH, Ng L, Miller JA, et al. An anatomically comprehensive atlas of the adult human brain transcriptome. Nature. 2012;489: 391–399. doi:10.1038/NATURE11405

28. Lotter LD, Dukart J. JuSpyce - a toolbox for flexible assessment of spatial associations between brain maps. 2022. doi:10.5281/zenodo.6884932

29. Romano M, Cacciatore A, Giordano R, La Rosa B. Postpartum period: three distinct but continuous phases. J Prenat Med. 2010;4: 22–5. Available: /pmc/articles/PMC3279173/

30. Pletzer B, Harris T-A, Scheuringer A, Hidalgo-Lopez E. The cycling brain: menstrual cycle related fluctuations in hippocampal and fronto-striatal activation and connectivity during cognitive tasks. Neuropsychopharmacology. 2019;44: 1867–1875. doi:10.1038/s41386-019-0435-3

31. Macoveanu J, Henningsson S, Pinborg A, Jensen P, Knudsen GM, Frokjaer VG, et al. Sex-steroidhormone manipulation reduces brain response toreward. Neuropsychopharmacol 2016 414. 2015;41: 1057–1065. doi:10.1038/npp.2015.236

32. Cutler AJ, Mattingly GW, Maletic V. Understanding the mechanism of action and clinical effects of neuroactive steroids and GABAergic compounds in major depressive disorder. Transl Psychiatry. 2023;13: 228. doi:10.1038/s41398-023-02514-2

33. Steiner M, Dunn E, Born L. Hormones and mood: From menarche to menopause and

beyond. J Affect Disord. 2003;74: 67–83. doi:10.1016/S0165-0327(02)00432-9

34. Oatridge A, Holdcroft A, Saeed N, Hajnal J V., Puri BK, Fusi L, et al. Change in brain size during and after pregnancy: study in healthy women and women with preeclampsia. Am J Neuroradiol. 2002;23: 19–26. Available: http://www.ncbi.nlm.nih.gov/pubmed/11827871

35. Luders E, Kurth F, Gingnell M, Engman J, Yong E-L, Poromaa IS, et al. From baby brain to mommy brain: Widespread gray matter gain after giving birth. Cortex. 2020;126: 334–342. doi:10.1016/j.cortex.2019.12.029

36. Martínez-García M, Paternina-Die M, Barba-Müller E, de Blas DM, Beumala L, Cortizo R, et al. Do Pregnancy-Induced Brain Changes Reverse? The Brain of a Mother Six Years after Parturition. Brain Sci. 2021;11: 1–14. doi:10.3390/BRAINSCI11020168

37. Rocchetti M, Radua J, Paloyelis Y, Xenaki L, Frascarelli M, Caverzasi E, et al. Neurofunctional maps of the 'maternal brain' and the effects of oxytocin: A multimodal voxel-based meta-analysis. Psychiatry Clin Neurosci. 2014;68: 733–751. doi:10.1111/pcn.12185

38. Morawetz C, Bode S, Derntl B, Heekeren HR. The effect of strategies, goals and stimulus material on the neural mechanisms of emotion regulation: A meta-analysis of fMRI studies. Neurosci Biobehav Rev. 2017;72: 111–128. doi:10.1016/j.neubiorev.2016.11.014

39. Whitfield-Gabrieli S, Nieto-Castanon A. Conn: a functional connectivity toolbox for correlated and anticorrelated brain networks. Brain Connect. 2012;2: 125–141.

40. Abraham A, Pedregosa F, Eickenberg M, Gervais P, Mueller A, Kossaifi J, et al. Machine learning for neuroimaging with scikit-learn. Front Neuroinform. 2014;8. doi:10.3389/fninf.2014.00014

41. Notter M, Gale D, Herholz P, Markello R, Notter-Bielser M-L, Whitaker K. AtlasReader: A Python package to generate coordinate tables, region labels, and informative figures from statistical MRI images. J Open Source Softw. 2019;4: 1257. doi:10.21105/joss.01257

42. Seabold S, Perktold J. Statsmodels: Econometric and Statistical Modeling with Python. 2010. pp. 92–96. doi:10.25080/Majora-92bf1922-011

43. Vallat R. Pingouin: statistics in Python. J Open Source Softw. 2018;3: 1026. doi:10.21105/JOSS.01026

44. Markello RD, Arnatkeviciute A, Poline J-B, Fulcher BD, Fornito A, Misic B. Standardizing workflows in imaging transcriptomics with the abagen toolbox. Elife. 2021;10. doi:10.7554/eLife.72129

45. Markello RD, Hansen JY, Liu Z-Q, Bazinet V, Shafiei G, Suárez LE, et al. Neuromaps: structural and functional interpretation of brain maps. Nat Methods. 2022;19: 1472–1479. doi:10.1038/s41592-022-01625-w

46. Hunter JD. Matplotlib: A 2D Graphics Environment. Comput Sci Eng. 2007;9: 90–95. doi:10.1109/MCSE.2007.55

47. Waskom M. seaborn: statistical data visualization. J Open Source Softw. 2021;6: 3021. doi:10.21105/joss.03021

48. Friston KJ, Williams S, Howard R, Frackowiak RSJ, Turner R. Movement-Related effects in fMRI time-series. Magn Reson Med. 1996;35: 346–355. doi:10.1002/mrm.1910350312

49. Schaefer A, Kong R, Gordon EM, Laumann TO, Zuo X-N, Holmes AJ, et al. Local-

Global Parcellation of the Human Cerebral Cortex from Intrinsic Functional Connectivity MRI. Cereb Cortex. 2018;28: 3095–3114. doi:10.1093/cercor/bhx179

50. Tian Y, Margulies DS, Breakspear M, Zalesky A. Topographic organization of the human subcortex unveiled with functional connectivity gradients. Nat Neurosci. 2020;23: 1421–1432. doi:10.1038/s41593-020-00711-6

51. Eklund A, Nichols TE, Knutsson H. Cluster failure: Why fMRI inferences for spatial extent have inflated false-positive rates. Proc Natl Acad Sci. 2016;113: 7900–7905. doi:10.1073/pnas.1602413113